# Apolipoprotein E–low density lipoprotein receptor binding: Study of protein–protein interaction in rationally selected docked complexes

**ARTICLE** *in* PROTEINS STRUCTURE FUNCTION AND BIOINFORMATICS · JUNE 2004

Impact Factor: 2.63 · DOI: 10.1002/prot.20080 · Source: PubMed



**2 AUTHORS:**

Martine Prévost
Université Libre de Bruxelles
**65** PUBLICATIONS **941** CITATIONS
SEE PROFILE

Vincent Raussens
Université Libre de Bruxelles
**68** PUBLICATIONS **1,878** CITATIONS
SEE PROFILE

PROTEINS: Structure, Function, and Bioinformatics 55:874–884 (2004)

# Apolipoprotein E-low Density Lipoprotein Receptor Binding: Study of Protein–Protein Interaction in Rationally Selected Docked Complexes

**Martine Prévost[1]* and Vincent Raussens[2]**
[1]*Bioinformatique génomique et structurale, Université Libre de Bruxelles, av. F. Roosevelt 50, B-1050 Brussels, Belgium*
[2]*Structure and Function of Biological Membranes, Université Libre de Bruxelles, av. F. Roosevelt 50, B-1050 Brussels, Belgium*

***ABSTRACT*** **Apolipoprotein E (apoE) is an important protein involved in lipid metabolism due to its interaction with members of the low-density lipoprotein receptor (LDLR) family. To further understand the molecular basis for this receptor-binding activity, an apoE fragment containing the receptor binding region (residues 135–151) was docked onto the fifth LDLR ligand binding repeat (LR5) by computational methods. A subset of structures generated by the docking was rationally selected on the grounds of experimental data combined with modeling and was used for further analysis.**

**The application and comparison of two different experimental structures for the apoE fragment underlines the local structural changes occurring in apoE when switching from a receptor-inactive to a receptor-active conformation. The body of interactions occurring at the interface between the two proteins is in very good agreement with the biochemical data available for both apoE and LDLR. Charged residues are involved in numerous ionic interactions and might therefore be important for the specificity of the interaction between apoE and LR5. In addition, the interface also features a tryptophan and a stacking of histidine residues, revealing that the association between the two proteins is not entirely governed by ionic interactions. In particular, the presence of histidine residues in the interface gives a structural basis for the pH-regulated release mechanism of apoE in the endosomes. The proposed molecular basis for apoE binding to LDLR could aid the design of strategies for targeting alterations in lipid transport and metabolism. Proteins 2004;55:874–884.** © 2004 Wiley-Liss, Inc.

**Key words: low-density lipoprotein receptor (LDLR); protein–protein interaction; docking; free energy of binding; lipid metabolism**

## INTRODUCTION

The low-density lipoprotein receptor (LDLR) is the primary mechanism for the uptake of plasma cholesterol into cells.[1]. The amino-terminal domain of the LDLR, which consists of seven repeated modules of 40 to 45 residues, mediates the binding of ligands to the lipoproteins. The three-dimensional structures of several of these ligands show similar features, such as three disulfide bonds and a high affinity calcium-binding site.[2–6]

Human apolipoprotein E (apoE), which stabilizes lipoprotein particles, plays an important role in regulating cholesterol homeostasis as well as in regulating plasma triglyceride clearance through its interaction with members of the lipoprotein receptor family such as LDLR.[7,8] ApoE is composed of two structurally and functionally independent domains.[9,10] The N-terminal domain contains the LDLR-binding region located in the vicinity of residues 136–150.[8] This region is rich in basic amino acids, which have been shown to be critical to receptor binding activity.[11,12] In the absence of lipids, apoE does not recognize LDLR, whereas when apoE or its N-terminal domain is complexed to lipids it binds efficiently to the receptor.[13] The three-dimensional structure of the N-terminal domain (residues 1–191) in its lipid-free form has been mapped at high resolution using X-ray crystallography.[14] This domain adopts a four-helix bundle in which the nonpolar faces of the helices are directed toward the center of the bundle. The interaction of apoE with lipids is believed to occur by the opening of the four-helix bundle, exposing the hydrophobic residues and thereby favoring binding to the acyl chains of the lipid molecules.[8,15,16]

Evidence suggesting that the basic residues of the receptor binding site of apoE are involved in ionic interactions with acidic residues includes the presence of highly conserved acidic residues in the LDLR repeated modules, the results of a study on the binding of an antibody mimetic of LDLR to apoE[17] and the high affinity of apoE for cell surface heparan sulfate proteoglycans.[18] However,

*Abbreviations:* ApoE, apolipoprotein E; CR, complement repeat; FDPB, finite difference to the Poisson–Boltzmann equation; GB, generalized Born model; LDL, low density lipoprotein; LDLR, low density lipoprotein receptor; LR5, fifth ligand binding repeat; LRP, low density lipoprotein receptor related protein; VLDL, very low density lipoprotein.

*Correspondence to: Martine Prevost, Bioinformatique génomique et structurale, Université Libre de Bruxelles, av. F. Roosevelt 50, B-1050 Brussels, CP165/61 Belgium. E-mail: mprevost@ulb.ac.be.

Received 1 September 2003; Revised 24 November 2003; Accepted 8 December 2003

Published online 5 March 2004 in Wiley InterScience (www.interscience.wiley.com). DOI: 10.1002/prot.20080

at present no specific ionic residue pair interactions between apoE and LDLR have been pinpointed.

To elucidate the molecular mechanism of the apoE–LDLR interaction, it would be helpful to study the structure of the complex. An important step in the comprehension of LDLR-mediated lipoprotein endocytosis is a description at the molecular level of the specific interactions taking place between LDLR and the apolipoproteins at the surface of the lipoproteins. However, the structure of the complex is unknown. While a substantial amount of structural information is available for both the individual domains of LDLR and the N-terminal domain of apoE, one of the most important ligands of LDLR, obtaining a high-resolution structure of the LDLR–apoE complex is still awkward. In most cases, the crystallization of complexes is a difficult task. In this particular case, crystallization problems are enhanced by the fact that, in order to bind efficiently to LDLR, apoE needs to be in a lipidated form.[13] In this context, a theoretical prediction of the structure of the complex might provide important and practical information on the interactions occurring between the two proteins.[19] Predicting protein–protein or peptide–protein docking, however, remains one of the more challenging tasks of structural biology. These systems have a multidimensional conformational space, which is difficult to sample exhaustively. The main problems are (i) enumerating possible docking orientations at a high resolution, (ii) considering the mobility of the docking surfaces and structural rearrangements upon interaction and (iii) reliably estimating the binding free energies of the docked states.

An approach that rationally combines a series of computational methodologies to predict the structure of the complex from two unbound molecules in a condensed phase was used here to predict the interaction of the 135–151 portion of apoE with the fifth repeated module of LDLR (LR5). The former was chosen as it contains the main LDLR binding region of apoE[8] and the latter is the principal mediator of the binding of LDLR to apoE.[20] The docking procedure was performed using two different three-dimensional structures of the apoE fragment, which depict the lipid-free[21] and lipid-associated[22] forms of the protein.

The 17-residue fragment of apoE is a ligand with a large number of degrees of freedom, which makes use of flexible ligand docking intractable in a first stage. Hence the following strategy was used. First, a rigid-body search was performed to find candidate structures. The collection of structures was condensed using biological information. The rigid-body association of two unbound molecules may at first seem like a rough assumption. However, it has been found that protein–protein association often involves only modest conformational changes,[23,24] suggesting that a rigid-body approximation might be applicable in many cases. Moreover, a recent nuclear magnetic resonance (NMR) investigation of CR3,[25] a complement-like repeat of the low density lipoprotein receptor related protein (LRP), in the presence of the receptor binding domain of human α2-macroglobulin has shown that the interaction of these two proteins does not induce large perturbations and therefore does not induce a conformational change within the CR3 domain. Because (i) CR3 is related to LR5 (>40% sequence identity and same overall fold), (ii) apoE is a ligand of LRP and (iii) α2-macroglobulin, like apoE, binds to LRP through a cluster of basic amino acids (K1370, K1374, and R1378),[26,27] we can postulate that in our complexes, the interaction between apoE and LR5 should not induce large perturbations in the proteins involved. Nevertheless to account for a possible rearrangement of the protein conformations, flexibility in the protein backbones and side chains was introduced using molecular dynamics in a later stage involving complexes representative of the selected structures. Local structural changes occurring in the lipid-associated form of apoE were shown to be essential to produce a satisfactory complex. The interfaces of a subset of rationally selected structures were examined to identify the interactions between the two molecular partners, and their relative binding free energy was estimated using a continuum electrostatic model. One structure was shown to be in good agreement with the large body of biochemical data on apoE mutants, as well as with structural data on an apoE–antibody[28] complex and on the endosomal conformation of LDLR.[29]

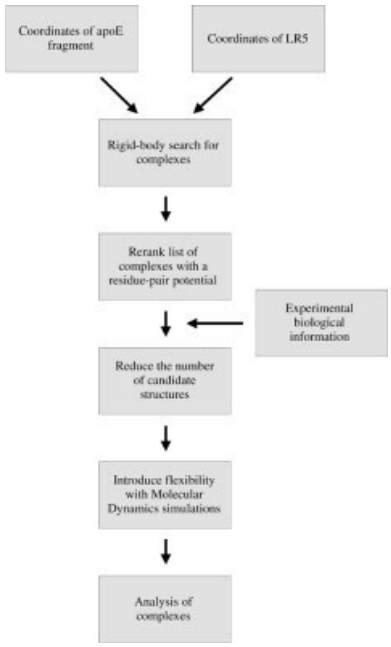


Fig. 1. The different stages of the docking protocol applied to the unbound coordinates of 135–151 apoE fragment and the fifth ligand binding repeat (LR5) of LDLR.

## MATERIALS AND METHODS

### Rigid-Body Docking

The docking protocol was carried out in a three-stage approach (Fig. 1). FTDOCK[30] was used to perform the rigid-body docking stage. This method consists of a global search of rotational and translational space. Complexes are scored on the basis of a function accounting for shape complementarity and favorable electrostatic interactions.

This function must account for possible conformational changes that can indeed occur upon binding. As shape complementarity is not usually sufficient to discriminate among the large number of docked molecules, the structures resulting from the global search were re-scored with an empirical potential derived using the statistics of residue–residue contacts across the interfaces of complexes from the Protein Data Bank.[31]

### Rational Selection of Complexes

In the next stage, available biological information about the location of the interface was used to reduce the number of candidate structures generated in the rigid-body docking procedure. Complexes with similar interfaces were clustered on the basis of a similar pattern of interactions, and representative structures were selected.

### Molecular Dynamics Simulation

To take into account the flexibility of both molecular partners upon binding, molecular dynamics simulations of the selected structures were performed. The simulations were completed using the CHARMM program.[32] The proteins interacted via the CHARMM 19 force field, where all heavy protein atoms and polar hydrogens are explicitly represented. The solvent was described as an approximate continuum by the generalized Born model.[33] This approach requires the use of a single dielectric constant to depict the implicit solvent. However, the surroundings of the protein–protein complex are not homogeneous. ApoE is known to bind to LDLR in a lipid-associated form; therefore an apolar environment circumscribes the apoE side of the complex. The chemical environment on the LR5 side of the complex is less clearly defined but is likely to be more polar. A dielectric constant of 4 was chosen in the simulations, thereby favoring the choice of a low-dielectric condensed phase.

### Calculation of Free Energy of Binding

The relative binding free energies of the predicted complexes were computed as follows using two computational methodologies. The calculations consisted of the computation of the van der Waals interaction between the two molecular partners and the electrostatic component of binding, which includes the electrostatic interaction between the two molecules and the desolvation cost for the individual molecules. The CHARMM force field was used to compute the van der Waals interaction. The electrostatic solvation component of the free energy of binding was computed using two different approaches. One method makes use of the program UHBD,[34] which solves the Poisson–Boltzmann numerically. This approach is based on the continuum model, wherein the solvent is described as having a continuous dielectric constant $\epsilon_{ext}$. The interior of the proteins is assigned an internal dielectric $\epsilon_{int}$ of 4, taking into account the electronic polarizability of protein atoms. The second approach estimates the electrostatic solvation contribution using the generalized Born model as implemented in CHARMM,[31] which provides an approximate continuum solvent representation described by a continuous dielectric constant $\epsilon_{ext}$. As in the molecular dynamics simulations, the problem of the choice of a value for $\epsilon_{ext}$ arises, as the external chemical environment of the complexes is not homogeneous. In these calculations, one could afford to use two extreme values, 4 and 80, describing respectively an apolar medium subjected to electronic polarizability and an aqueous solution. The coulombic interaction component was computed with UHBD and CHARMM respectively in the first and second approaches. In the UHBD calculations, a contribution accounting for the nonpolar solvation free energy, which is assumed to be proportional to the loss of solvent-accessible surface area, was included.

### pKa Calculation

A continuum dielectric model was used to calculate the pKa values of K143 and K146 in the 135–151 fragment of the crystal and NMR structures. In the present study, the UHBD program with an interface to CHARMM[35] was employed. The calculations were completed assuming an internal dielectric constant of 20.[36]

### Electrostatic Potential

The electrostatic potential was determined on the high-resolution crystal structure of the unbound LR5[4] using the Poisson–Boltzmann equation.[37] The dielectric constant inside the protein was set to 4, and the dielectric constant in the solvent was set to 80. A 0.15*M* salt concentration was assumed. All charges of the protein and the calcium ion were included in the calculation.

### Contact and Solvent Accessible Areas

The contact area between residues of the apoE fragment and LR5 was computed as the sum of the polyhedral faces that atoms of a given residue pair have in common. The polyhedra calculation was performed using a method based on the radical planes implemented in the program SurVol.[38] The solvent-accessible surface area was computed from atomic coordinates of the crystal and NMR structures of the 135–151 apoE fragment with a probe radius of 1.4 Å and using the analytical procedure of SurVol as implemented in the BRUGEL package, respectively.[39]

## RESULTS AND DISCUSSION

A rigid-body docking protocol, as described in Materials and Methods and Figure 1, has been applied to the high-resolution coordinates of LR5[4] and an apoE fragment spanning residues 135–151. Two different sets of coordinates of the apoE fragment were used. One was extracted from the crystal structure of the N-terminal domain (residues 1–191)[21] (PDB # 1NFN) and was expected to correspond to the lipid-free form of this apoE domain. The other set was taken from the representative structure of the most populated conformational ensemble of the apoE (126–183) peptide determined by NMR in the presence of a lipid-mimetic agent[22] and thought to be representative of the lipid-bound form. Both structures adopt a helical conformation in the 135–151 portion. However, the root-

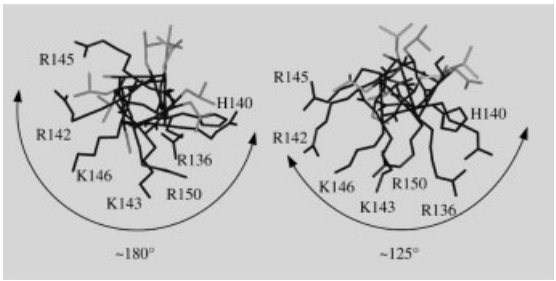


Fig. 2. Representation down the helix axis of the 135–151 portion of apoE as extracted from (left panel) the crystal structure (PDB # 1NFN,[21]) (right panel) the representative structure of the most populated NMR conformational ensemble of apoE (126–183) determined in a lipid-mimicking agent.[22] Side chains of basic amino acids are depicted as black sticks. Other side chains are shown in light grey. Arcs delineate the faces of the helices occupied by the basic amino acids with the exception of R145, which stands apart.

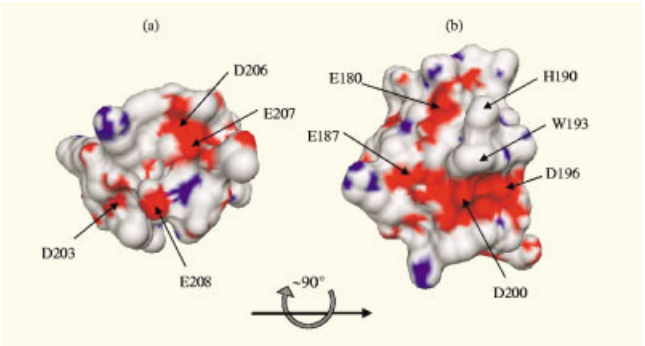


Fig. 3. Electrostatic potential mapped onto the solvent-accessible solid surface computed on the fifth ligand binding repeat (LR5) of LDLR. Red and blue colors indicate negative and positive electrostatic potentials respectively. Two different faces featuring patches of negative electrostatic potential are shown: (a) face 2 (f2) contains D203, E208 and two other calcium-binding residues, D206 and E207; (b) face 1 (f1) contains E180, E187 and two calcium-binding acidic residues, D196 and D200.

mean square difference for the Cα positions between the two structures was 1.3 Å, indicating a substantial structural difference for a fragment of 17 residues in length.

The list of complexes generated by rigid-body docking was re-scored using a residue-pair potential. This stage was performed because previous studies indicated that scores based mainly on surface complementarity tend to favor incorrectly docked complexes.[19]

To constrain the number of possible complex structures, the re-scored list of predicted complexes was then condensed in a two-step process using the available biochemical information on both apoE and LR5. The first step consisted of selecting the complexes having certain apoE basic amino acids (R136, H140, R142, K143, K146 and R150) within a distance of 4.5 Å from any LR5 residue. Mutational data indicate that these residues, located on the hydrophilic face of the amphipathic helix (Fig. 2), are most likely to be involved in binding.[8,40,41] In a second stage, the list of complexes remaining after the first stage was further edited by requiring all complexes to have either (i) the acidic residues E180, E187, D196 and D200 or (ii) D203, D206, E207 and E208 of LR5 within a distance of 4.5 Å from any residue of the apoE fragment. The different sets of acidic residues were suggested by their location on two different faces of the molecular surface of LR5. The overall architecture of LR5 consists roughly of three faces. One is concave, composed mainly of hydrophobic and aromatic residues and, in accordance with the electrostatic potential, is approximately neutral. As shown by the solvent-accessible solid surface (Fig. 3), two other faces, which will be referred to hereafter as to f1 and f2, present patches of negative electrostatic potential. As ligand–receptor recognition is likely to issue from ionic interactions, only f1 and f2 were considered for further examination. The f1 face [Fig. 3(b)] accommodates four acidic residues, E180, E187, D196, and D200. D196 and D200 side chains bind the LR5 calcium ion; nevertheless, these side chains retain some accessibility from the surface. The f2 face [Fig. 3(a)] also harbors four acidic residues, D203, E208, D206, and E207. The latter two acidic residues' backbones line the surface, while their side chains are buried, engaged in calcium ion coordination.

With the apoE (135–151) fragment extracted from the lipid-free crystal structure,[21] there were zero and three complexes found to fulfill the biochemical requirements for faces f1 and f2, respectively. Furthermore, among the three structures involving the f2 face, none had a positive residue-pair potential-based scoring (see Materials and Methods and Fig. 1). The structural docking predictions thus suggest that the crystal structure of the 135–151 apoE fragment does not permit the formation of a complex that complies with the imposed requirements. For the apoE (135–151) fragment extracted from the NMR structure,[22] there were 11 and 18 complexes found to fulfill the biochemical requirements for faces f1 and f2, respectively. Hence, in the following sections we limit the analysis of the selected conformers to those generated with the apoE NMR structure. The 11 f1 structures all presented a positive scoring, while only eight of the 18 f2 complexes presented a positive scoring. The interfaces of these 11 f1 and eight f2 structures were further examined to identify possible ionic interactions between the molecular partners. Indeed, the selection protocol that favored complexes featuring a charged interface did not guarantee that the latter would display specific ionic interactions involving residue pairs from apoE and LR5. Four of the 11 f1 structures were then selected for further study because they are representative of different patterns of electrostatic interaction, which are listed in Table I. Among the eight f2 structures, after elimination of those that feature no ionic interaction, only one representative structure was selected.

Figure 4 shows the interfaces of two predicted LR5–apoE complexes, one for each LR5 face. In the complexes involving the f1 face, the calcium binding loops dock on the hydrophilic face of the apoE helix, in contrast to the f2 structure wherein the calcium binding loops are not involved. The four representative f1 complexes can be roughly divided into two categories. In the first category, the apoE helix axis, starting at its N-terminus, runs from the LR5 E180/E187 location towards the calcium-binding site. Complexes f1-II and f1-IV fit this description. In the second

**TABLE I. Interactions Formed at Interfaces of Five Selected Models Between the Basic Amino Acid Side Chains of 135–151 apoE Fragment and Fifth Ligand Binding Repeat (LR5) of LDLR[a,b]**

| ApoE f1-I | | |
|---|---|---|
| ApoE | LR5 | Type of Interaction |
| R136 | P199-O/K202-O | Hydrogen bonds |
| R142 | W193 | Amino–aromatic |
| K143 | D200 | Salt bridge |
| R147 | E180 | Salt bridge |
| **ApoE f1-II** | | |
| ApoE | LR5 | Type of Interaction |
| R136 | G185-O | Hydrogen bond |
| H140 | E180 | Longer-range ion pair |
| K143 | E187 | Salt bridge |
| K146 | D200/D196 | Salt bridge/longer-range ion pair |
| | W193 | Amino–aromatic |
| R150 | S192-O | Hydrogen bonds |
| **ApoE f1-III** | | |
| ApoE | LR5 | Type of Interaction |
| R136 | E207 | Salt bridge |
| | G197/E207-O/C210-O | Hydrogen bonds |
| H140 | D196 | Salt bridge |
| K143 | D196 | Longer-range ion pair |
| K146 | E180 | Longer-range ion pair |
| | S191 | Hydrogen bond |
| R150 | E180 | Longer-range ion pair |
| **ApoE f1-IV** | | |
| ApoE | LR5 | Type of Interaction |
| R136 | E180 | Salt bridge |
| H140 | H190 | Stacking |
| R142 | E187 | Longer-range ion pair |
| | D200-O/C201-O | Hydrogen bonds |
| K143 | E187 | Salt bridge |
| | C188-O | Hydrogen bond |
| K146 | D196/D200 | Salt bridges |
| | W193 | Amino–aromatic |
| R150 | S192-O/C195-O | Hydrogen bond |
| ***ApoE f2*** | | |
| ApoE | LR5 | Type of Interaction |
| R142 | E208 | Salt bridge |
| K143 | E208 | Salt bridge |

[a]Interactions were identified with a distance criterion only. For hydrogen bonds and salt bridges: distance donor–acceptor or nitrogen–oxygen ≤3.5 Å; for longer-range ion pairs: distance nitrogen– oxygen ≤6 Å; for amino-aromatic nitrogen-ring center distance ≤5 Å. Histidine–histidine stacking distance = 3.8 Å.

[b]Interactions involve side chains of apoE residues with side chains (when no atoms are mentioned) or backbone atoms of LDLR.

category, the apoE helix axis is roughly rotated by 180° relative to the first category structures with the helix N-terminus sitting on top of the calcium-binding site. This category contains structures f1-I and f1-III. Within each

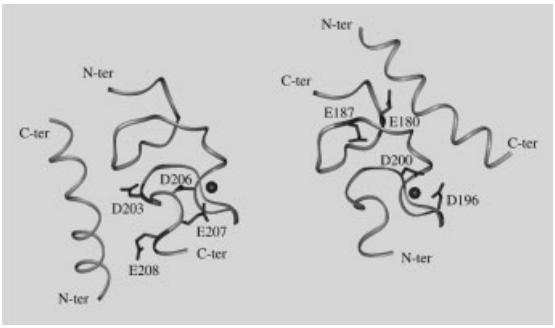


Fig. 4. Ribbon diagrams of two predicted complexes resulting from different filtering steps in the docking protocol (see text). The helical ribbon depicts 135–151 apoE fragment. The other ribbon is LR5, and the calcium ion is shown as a sphere. The interface of complex f2 is shown on the left, and complex f1-IV is shown on the right. Its interface contains the calcium binding site loops and four acidic residues, E180, E187, D196 and D200. Acidic side chains are shown in a stick representation.

category, the differences between the complexes are due to a translation along the helix axis with regard to the LR5 surface.

At this stage, we abandoned the rigid-body approximation and introduced flexibility in protein side chains and backbone for both LR5 and apoE fragment. The five representative complexes were subjected to 500ps-molecular dynamics simulations with an implicit description of the solvent. The last structure of each trajectory was then minimized and searched for interactions of the apoE basic amino acid side chains able to explain a possible association.

The interactions formed at the interfaces of the five complexes are listed in Table I. One notices that the f2 structure participates in significantly fewer interactions than do the f1 structures. Among the f1 structures, complex I participates in the smallest number of interactions. The consequences of a smaller number of interactions are not evident, as the different interactions may vary in their contribution to binding. Hence, in attempt to make a quantitative estimate of the strength of the association between the two molecules, the relative binding free energy for the five complexes was computed (Table II). These estimates were designed to be valid for the relative binding energies of a given complex system. They neglect terms such as the configurational, rotational and translational entropy that contribute to the relative binding of different ligands and to the absolute binding energy because these terms are expected to be similar for a given system in different structural associations. Two different calculations were run. In one calculation, the electrostatic component of solvation was computed using the generalized Born model (GB); in the other, it was computed by the finite difference from the Poisson–Boltzmann equation (FDPB) (see Materials and Methods). These two methods describe the medium external to the complex as a continuum dielectric solvent. Here, as in the real system, the external medium surrounding the complex is not homogeneous. A lipid phase lines apoE on one side, while the phase flanking the LR5 surface and not in contact with apoE is likely to be more polar. Hence two extreme limit

**TABLE II. Relative Free Energy of Binding Computed Using Two Different Methodologies to Evaluate Electrostatic Solvation Component and Contact Area (Å$^2$) Between apoE Fragment and LR5**

A. Calculation using the generalized Born equation

| Complex | Contact Area (Å$^2$) | $\Delta G$ ($\varepsilon_{ext}$ = 4) | $\Delta G$ ($\varepsilon_{ext}$ = 80) |
|---|---|---|---|
| ApoE f1-I | 492 | −265.0 | −52.3 |
| ApoE f1-II | 423 | −243.8 | −29.0 |
| ApoE f1-III | 500 | −278.8 | −65.8 |
| ApoE f1-IV | 538 | −302.7 | −67.6 |
| ApoE f2 | 436 | −233.5 | −30.7 |

B. Calculation using the finite difference to the Poisson-Boltzmann equation[a]

| Complex | $\Delta G$ ($\varepsilon_{ext}$ = 4) i.f. = 0 m*M* | $\Delta G$ ($\varepsilon_{ext}$ = 4) i.f. = 145 mM | $\Delta G$ ($\varepsilon_{ext}$ = 80) i.f. = 0 m*M* | $\Delta G$ ($\varepsilon_{ext}$ = 80) i.f. = 145 m*M* |
|---|---|---|---|---|
| ApoE f1-I | −271.0 | −125.2 | −48.0 | −42.7 |
| ApoE f1-II | −259.3 | −112.3 | −34.1 | −29.0 |
| ApoE f1-III | −285.8 | −137.3 | −61.4 | −57.2 |
| ApoE f1-IV | −305.2 | −153.4 | −58.1 | −52.6 |
| ApoE f2 | −249.8 | −104.7 | −42.4 | −37.4 |

[a]Internal dielectric constant of complex = 4.

values of dielectric constants were used to describe the external medium. The first described the medium as one of low dielectric constant ($\epsilon_{ext}$ = 4), depicting the acyl chains of lipids. The other value corresponds to a high dielectric constant ($\epsilon_{ext}$ = 80), characterizing an aqueous solution. In the finite difference to the Poisson–Boltzmann equation (FDPB) calculation, two values for ionic strength were used. A salt concentration of zero was one of the two values; the other (145 m*M*) was chosen to correspond to a physiological concentration.

The ΔG values computed with GB match quite well those computed with FDPB. At an $\epsilon_{ext}$ value of 4, the electrostatic contribution is mainly coulombic, which favors the binding, while at an $\epsilon_{ext}$ value of 80 there is a strong solvation component that opposes the complex association. Increasing the ionic strength predictably disfavors the binding. In most cases, the ΔG values suggest that structure f1-IV (see Fig. 5) is the most strongly associated complex, followed closely by complex f1-III. However, the ΔG computed by FDPB with an $\epsilon_{ext}$ value of 80 slightly favors complex f1-III over complex f1-IV. Complex with the f2 face forms the least favorable association in all calculations, but the estimation performed at an $\epsilon_{ext}$ value of 80 for f1-II showed the least stable interface. The contact area values computed between apoE and LR5 residues for each complex (Table IIA) correlate well with the ΔG values.

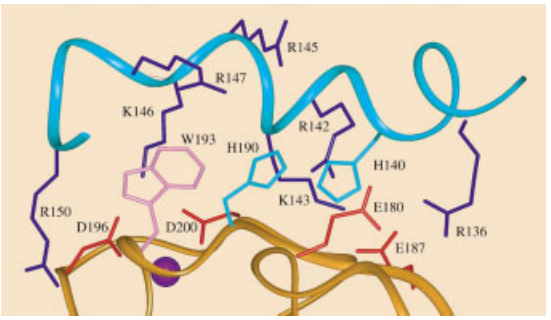


Fig. 5. A detailed view of the predicted interactions at the interface of the most favorable modeled complex, f1-IV. Backbone is shown as a ribbon diagram in cyan for apoE and in orange for LR5. Side chains involved in the interface are depicted as sticks. Basic and acidic amino acids are colored in blue and red respectively. Histidines and tryptophan are shown in cyan and pink respectively.

## Discussion

The presence of highly conserved acidic residues within the lipoprotein receptor (LR) modules and the positively charged region of apoE (residues 136–150) has led to the hypothesis that ligand–receptor recognition is due to electrostatic interactions. The apoE fragment can electrostatically interact with LR5 through its hydrophilic face, which contains basic amino acids known to be important for receptor binding. A careful check of the electrostatic potential at the surface of LR5 showed that, in the presence of a calcium ion, two different regions of LR5 harbor a negative potential, defining two faces where apoE can potentially bind, referred to as f1 and f2 (see Results and below). These criteria, applied to both apoE and LR5, were used to further select the most favorable apoE–LR5 docked complexes, in which the basic region of apoE is in close proximity to one of the two negatively-charged faces of LR5.

### *Lipid-Associated Versus Lipid-Free Form of ApoE*

In our docking experiments, we used two different apoE structures. One fragment was extracted from an X-ray crystal structure of the N-terminal domain of apoE,[21] and the other came from the NMR structure of an apoE peptide, determined in the presence of a lipid-mimetic agent.[22] We used these two fragments as representative of the lipid-free and the lipid-bound conformations of apoE

respectively. A first important result of our docking experiments is that we were able to predict the formation of apoE–LDLR interfaces that complied with the available biochemical information only with the apoE NMR structure. The X-ray structure produced either no complex or complexes with unfavorable scoring values. It is well known that apoE or its N-terminal domain is able to interact with the LDLR only when complexed with lipids.[13] The fact that only the NMR structure of the apoE fragment produces acceptable complexes with LR5 indicates that our docking procedure is able to distinguish between the two apoE conformations. The structural differences between the lipid-free and lipid-associated forms may explain this result, which is in agreement with the view that the multiple basic residues in the 136–150 apoE fragment may require a particular orientation for optimal receptor binding activity.[40] Superposition of the two structures results in a significant root-mean square deviation of the Cα atomic positions and shows a significantly different curvature. Moreover, in the NMR structure, the basic amino acids are less scattered, forming a better aligned and more elongated hydrophilic face (see Fig. 2). A recent NMR study[42] showed that, upon binding to dimyristoylphosphatidylcholine vesicles, the solvent accessibilities of K143 and K146 were increased and the pKa values of the same two residues were significantly lowered. In the absence of lipids, Lund-Katz and her coworkers[42] estimated the pKa of K143 and K146 to be respectively equal to 10.1 and 10.4, close to the normal pKa value of a fully hydrated lysine, while in the presence of lipids these values dropped respectively to 9.5 and 9.2. We calculated the surface accessibility of the hydrophilic face of the two apoE fragments we used. In the computation, we included R136, H140, R142, K143, K146, and R150, residues likely to be involved in binding with LR5 (see below and Table I). Using these residues, the accessible surface for the fragment extracted from the X-ray structure represents 910 Å$^2$, while for the NMR structure the accessible surface is equal to 1114 Å$^2$. This represents a ≈20% increase in the accessibility of the hydrophilic face of apoE. A calculation of the pKa of K143 and K146 under both conditions showed that, in the absence of lipids (X-ray structure), the pKa values are respectively equal to 10.2 and 10.0, while in the presence of a lipid mimetic agent (NMR structure), these pKa values are equal to 9.9 and 9.6. Both of these calculations (accessible surfaces and pKa values) are in good agreement with Lund-Katz and coworkers' experimental results. They also corroborate a local increase in positive electrostatic potential and local structural changes upon lipid association in the 136–150 apoE region, and confirm that the NMR structure of apoE (126–183) in the presence of a lipid mimetic agent is probably a good model of the receptor active conformation of the receptor binding region of apoE, as has been previously stated.[22,43]

### *Free Energy of Binding*

Among the complexes formed by the apoE fragment and LR5, we selected five representative structures, four involving the f1 face and one involving the f2 face. The four models involving the f1 face differ by the relative position and/or orientation of the apoE fragment with respect to LR5. Theoretical calculations of the relative binding free energy were performed on the five representative structures. These calculations can account in a qualitative sense for the observed binding energies. However, accurate quantitative agreement is more difficult to obtain, in part because these calculations are sensitive to geometry and require highly accurate structures. The external dielectric constant, $\epsilon_{ext}$, is also a crucial variable associated with calculations of this type. In most calculations, a value of 80 is used, representing an aqueous solution. In our system, the external medium surrounding the apoE–LDLR complex was inhomogeneous, varying from an apolar to a highly polar environment, which made the use of a single value for $\epsilon_{ext}$ awkward. To circumvent this problem, two extreme values of $\epsilon_{ext}$, describing either an apolar medium or an aqueous solution, were used. Although the values of free energy of binding obtained did change drastically with $\epsilon_{ext}$, their relative values correlated quite well with the other parameters used to describe the different complexes [number of ionic and polar interactions (Table I), surface contact area (Table IIA)]. The favorable values of free energy of binding in the predicted complexes indicate that the desolvation effects, which are significant and unfavorable for complexes with highly charged and polar interfaces in an aqueous solution ($\epsilon_{ext}$ = 80), are more than compensated by the formation of networks of ion pairs, hydrogen bonds and polar as well as van der Waals interactions. In an apolar environment whose dielectric constant value is close to that in the complex, the desolvation component is negligible, and the electrostatic and van der Waals interactions favorably contribute to the free energy of binding.

### *Comparison with Mutants*

When looking at all of the parameters, including the number of interactions (Table I), the surface contact area (Table IIA) and the relative binding energy (Table II), two structures (f1-IV and f1-III) stand out from the five representative models. Because of this, we decided to restrict our description and discussion to these two, most favorable apoE–LR5 complexes.

Complexes were selected so that oppositely-charged surfaces of LR5 and apoE face each other. This is a necessary but not sufficient condition to guarantee that the complexes feature specific ionic interactions formed between the two molecular partners. It is thus essential to examine whether our predicted structures feature interactions that corroborate the experimental binding data for naturally occurring and site-directed mutants in the 136–150 apoE region.[8,40,41] The loss of the positive charge occurring in R136S mutant results in a decrease of about 60% of the binding activity. The two most favorable predicted complexes feature at least one salt bridge interaction between R136 and LR5. The substitution of H140 by Ala reduces the activity by about 50%. In complex f1-III, H140 forms a salt bridge with D196, while in f1-IV H140 forms a stacking with H190 coming from LR5. This

His-His stacking interaction might be important in the pH dependence of the apoE release from the LDLR (see below). R142 has a naturally occurring mutant that results in defective binding. Interactions between LR5 and R142 are formed only in complex f1-IV. R142 forms a long-range ionic interaction with E187 and also H-bonds with the backbone carbonyls of residues D200 and C201. The K143A substitution results in either an almost complete lack of binding or in a 75% drop, depending on the study. Complex f1-IV features one salt bridge between K143 and E187 and a hydrogen bond of K143 with C188. Complex f1-III displays a longer-range ionic interaction between K143 and D196. Substitution of K146 into Q reduces LDLR binding to about 30% of the wild-type value. Complexes f1-III and -IV feature either a longer-range ionic interaction or a salt bridge involving K146 and at least one LR5 residue. Interestingly, in f1-IV, K146 and W193 interact through an amino–aromatic interaction. The substitution of R150 into alanine reduces the binding activity by about 75%. Complexes f1-III and -IV display either ionic interactions or hydrogen bonds involving R150 and LDLR residues. No interaction involving R145 was identified in the modeled complexes, although a natural substitution affecting R145 results in defective binding. Figure 2 shows that R145, according to the crystal and NMR structures, is the only basic amino acid side chain that points in a direction opposite that of the hydrophilic face of the helix. Hence the explanation for the disagreement with the experimental data may be twofold: a reorientation of R145 side chain which has not been properly modeled occurs upon binding, and/or a structural perturbation produced by the natural mutation affects neighboring residues and/or salt bridges.

One cannot exclude the possibility that the reported substitutions, which decrease the receptor binding, could be due to conformational change instead of to the loss of a particular interaction. However, substitution of a neutral for a basic amino acid in the mutants K143A and K146Q was shown not to alter the α-helical structure of the N-terminal domain of apoE3 complexed to DMPC.[41] For other substitutions, R136S, H140A, R150A, a secondary structure prediction program[44] was run. No result predicted a helical disruption upon substitution (data not shown), suggesting that it is the loss of the basic amino acid that is important for the effect on binding.

Overall, the best candidate structures feature interactions compatible with the naturally occurring and site-directed mutations of basic amino acids. Most of the basic residues of apoE in the models are involved either in salt bridges, hydrogen bonds or other polar interactions with LR5 residues. The interfaces display multiple interactions between basic amino acids of apoE and residues of LR5. In that respect, these models are supported by experiments, which show that it is not a single but several basic amino acids of the 136–150 apoE region that contribute to binding. This is in perfect agreement with the current view that apoE binds to LDLR through electrostatic interactions.

### *Antibody Binding Model*

In the case of LR5, predicting the effects of natural or site-directed mutants is more difficult, because most of the mutations leading to familial hypercholesterolemia have been shown to produce misfolded binding repeat.[4,45] Nevertheless, the predicted complexes and the characteristics of their interfaces can be further examined in the light of a few available structures. A first interesting structure to examine and compare to our complexes is the modeled interface developed for the complex formed by apoE and the Fab fragment of a monoclonal antibody, 2E8, specific to the receptor binding region of apoE.[17] It has been demonstrated that 2E8 binds apoE with the same binding specificities for apoE isoforms as LDLR. 2E8 also prevents apoE from binding to LDLR.[28] The modeled interface, consistent with the binding properties of 2E8, reveals the critical role of electrostatic interactions and charge neutralization, in perfect agreement with the numerous ionic interactions present in our f1-III and f1-IV complexes. An intriguing point in the apoE–2E8 complex is the presence of a tryptophan residue (W50 from 2E8) in the interface, more or less facing the carbonyl position of apoE K146 (see Fig. 9 in ref. 17). Interestingly, in our f1-IV complex, K146 forms an amino–aromatic interaction with W193 coming from LR5. The interaction of aromatic residues with basic amino acids has been found to occur with some preference in proteins[46] and in some instances has been shown to provide a stabilizing contribution.[47] Moreover, the tryptophan side chain is found to H-bond either with the backbone of K143 or that of R150 in f1-III and f1-IV respectively. Further support for the possible importance of a tryptophan residue in the apoE–LR5 interface comes from the recent NMR structure of the third complement repeat of LRP,[25] previously mentioned. The most important residues involved in the CR3 α2-macroglobulin interaction are, in decreasing importance, Q20, W23, E21, D30, and F11.[25] If Q20 and E21 are not present in LR5, the three other residues are conserved and correspond to W193, D200 and F181 in LR5. While neither f1-III nor f1-IV displays an interaction with F181, both have ionic interactions with the previous residue, E180. While both complexes show interactions involving W193 (see above and Table I), only f1-IV displays a salt-bridge between D200 and K146 on apoE (Table I). A more recent study of CR5 and CR6 of LRP has confirmed, using mutagenesis, the critical role of the conserved tryptophan amino acid in the binding of the receptor-associated protein (RAP) to LRP. For reasons mentioned above for CR3 and because RAP, like apoE, is known to bind to all members of the LDLR family,[48,49] these experiments are more likely to be relevant to the description of the apoE–LR5 interface. The critical presence of a tryptophan residue on the binding face of different, related ligand binding repeats shows that the LR5 face most likely involved in ligand binding is the f1 face.

### *Endosomal LDLR Conformation*

Another structure that has been suggested to be relevant to the description of the apoE–LDLR interface is one

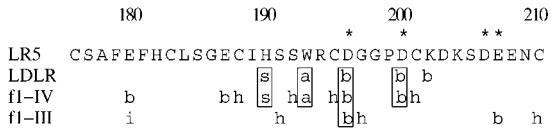


Fig. 6. Amino acid sequence of LR5. Residues with side chains that participate in calcium coordination are shown above the sequence using asterisks. Interactions of LR5 residues shown in the X-ray crystal structure with other portions of the extracellular domain of LDLR at pH 5.3[29] and with apoE in the best two predicted complexes are indicated below the sequence. The letters b, h, a, i and s stand for salt bridge, hydrogen bond, amino–aromatic, ionic and stacking interactions respectively. Boxed interactions are conserved in the crystal and at least one of the predicted models.

recently determined for the extracellular domain of LDLR.[29] This crystal structure, obtained at pH 5.3, represents the endosomal conformation of the LDLR. In this structure, ligand binding repeats LR4 and LR5 are held in place through interactions with the β-propeller motif of the receptor, while other repeats seem to be fixed by intermolecular crystal contacts. The authors suggest that, at endosomal pH, following release of the lipoprotein ligand, the β-propeller can act as an alternative substrate for the two ligand binding repeats. In this case, the interactions found between LR5 and the β-propeller might be the same or at least very similar to those found between LR5 and apoE. Despite the relatively low resolution of the structure, Rudenko and coworkers were able to clearly identify residues involved in the interaction among LR4, LR5 and the β-propeller. In the case of LR5, they found many salt bridges involving H190, D196, D200, and K202 with residues from the propeller domain. Interestingly, W193 forms interactions with two charged amino acids from the propeller. A cluster of histidines (H190, H562 and H586) was also found between LR5 and the propeller domain. All of these specific interactions can be compared to the ones we found in our predicted apoE–LR5 complexes (Fig. 6 and Table I). In the f1-III complex, among all of the above-cited residues, only D196 could be identified as forming a salt bridge with H140 and a long-range ionic pair with K143 (Table I). On the other hand, in the f1-IV apoE–LR5 complex, four out of the five residues of LR5 which were identified interacting with the propeller domain are involved in contacts with apoE. Importantly, these contacts are of the same type as those described by Rudenko et al.[29] between LR5 and the β-propeller. D196 and D200, two acidic residues engaged in the coordination of the calcium ion, are able to form salt bridges with K146 on apoE. W193, as previously mentioned, makes an amino–aromatic contact with K146, and, to our great surprise, we also identified a stacking of histidines (between H190 from LR5 and H140 from apoE) (Figs. 5 and 6). This strongly suggests that the f1-IV complex is the best candidate to describe the interactions that occur between apoE and LR5. Other elements reinforce this idea. In the f1-IV complex, apoE makes also two salt bridges with two other acidic residues on LR5, E180 and E187. These two amino acids are strictly conserved in LR5 from LDLR across species and also in the homologous repeat in the very low-density lipoprotein (VLDL) receptor. These two residues, not implicated in the interface between LR5 and the β-propeller, might therefore be important in the specificity of the interaction between apoE and LR5. The presence of a tryptophan and a stacking of histidines is another important feature. This shows that the contact between the two proteins is not entirely governed by ionic interactions. W193 is also strictly conserved among LDL and VLDL receptors. The importance of a tryptophan residue in different ligand binding repeats has been discussed above.

LDLR removes lipoproteins from plasma circulation via a receptor-mediated endocytosis. Ligands bound by LDLR are internalized and then released in the endosomes at a pH lower than 6. This mechanism has been suggested to be a pH-regulated reversible process[29] whose structural basis is unknown. The presence of an interaction between H140 from apoE and H190 in LR5 at a neutral pH, as in complex f1-IV, suggests a potential mechanism for apoE release at low pH. A distinctive feature of a histidine residue is that it can change its protonation state in the pH range 5–7.5 and, at acidic pH, is more likely to support a positive charge. Therefore the decrease in pH in the endosomes would trigger a repulsion between the two positively charged histidines and facilitate the ligand release. Both histidine residues are conserved across species. Mutation of H190 into a tyrosine has been described in familial hypercholesteriolemia patients,[50] suggesting functional importance for this amino acid.

### *Contribution from Other LR Repeats*

It should be noted that other repeats, located upstream from LR5, contribute as well, though to a lesser degree, to apoE binding to the receptor,[20] and it has been suggested that ligand-binding specificity may result from the rearrangement of two or more repeat modules.[5] This proposal is supported by the apoE (126–183) peptide conformation, a bent flexible helix which is about 70 Å long. This apoE fragment contains an additional region 171–183, which is important for receptor binding activity,[51] and could possibly interact with a second repeat.[22] When superimposing the entire apoE (126–183) peptide on the 135–151 fragment in complexes f1-III and f1-IV, the computed distances between the N-terminus of LR5, where the linker between LR4 and LR5 anchors, and R172 are ≈43 and ≈55 Å for complex f1-III and f1-IV respectively. This interaction would therefore be easier with complex f1-III, which has its N-terminal side oriented towards the R172-containing region of apoE. Nevertheless, when modeled in an extended conformation, the twelve-residue linker region between LR4 and LR5 separates the two repeats by about 38 Å at an uppermost estimate (data not shown). This distance, along with the diameter of a single repeat, which corresponds approximately to 25 Å, suggests that LR5–apoE association, as predicted in the f1-IV complex, may permit the interaction of LR4 with the region including R172 in the 126–183 apoE peptide. Moreover, it has been demonstrated that, in ligand binding repeat pairs, each individual repeat acts as an isolated module with few or no interactions between adjacent modules.[5,52] A dy-

namic analysis showed that the linker region between the LR5–LR6 pair is flexible, and the position of the two modules with respect to each other is not fixed.[53] Because the linker region between LR4 and LR5 is longer than between LR5 and LR6, one can expect that the LR4–LR5 pair has even more flexibility. The dynamics of the apoE (126–183) peptide also demonstrated a certain degree of flexibility for this region of apoE.[22] This shows that both proteins are probably malleable enough to permit the interaction of LR4 or another repeat with the apoE region around R172 even if LR5 is oriented as in the f1-IV complex.

In summary, in the course of our docking procedure applied to an apoE (135–151) fragment and LR5, we found that complex f1-IV represents the structure that best describes the interface between apoE and LR5. A description at the molecular level of the interactions that take place between the two proteins is in very good agreement with the biochemical data available for both apoE and LDLR. Charged residues in both apoE and LR5 are involved in numerous ionic interactions. In addition to charged residues, the interface also features a tryptophan and two histidines that might have important roles in the binding of apoE to LDLR. The presence of histidine residues in the interface between the two proteins gives a strong structural basis for the pH release of apoE in the endosomes.

## ACKNOWLEDGMENTS

We are grateful to Dr. Brian D. Sykes for kindly providing us with the NMR coordinates of the apoE (126–183) peptide in the presence of TFE. M.P. and V.R. are respectively senior research associate and research associate at the National Fund for Scientific Research (Belgium).

## REFERENCES

1. Brown MS, Goldstein JL. Heart attacks: gone with the century? Science 1996;272: 629.
2. Daly NL, Scanlon MJ, Djordjevic JT, Kroon PA, Smith R. Three-dimensional structure of a cysteine-rich repeat from the low-density lipoprotein receptor. Proc Natl Acad Sci USA 1995;92: 6334–6338.
3. Daly NL, Djordjevic JT, Kroon PA, Smith R. Three-dimensional structure of the second cysteine-rich repeat from the human low-density lipoprotein receptor. Biochemistry 1995;34:14474–14481.
4. Fass D, Blacklow SC, Kim PS, Berger JM. Molecular basis of familial hypercholesterolaemia from structure of LDL receptor module. Nature 1997;388:691–693.
5. North CL, Blacklow SC. Structural independence of ligand-binding modules five and six of the LDL receptor. Biochemistry 1999;38:3926–3935.
6. Clayton D, Brereton IM, Kroon PA, Smith R. Three-dimensional NMR structure of the sixth ligand-binding module of the human LDL receptor: comparison of two adjacent modules with different ligand binding specificities. FEBS Lett 2000;479:118–122.
7. Mahley RW. Apolipoprotein E: cholesterol transport protein with expanding role in cell biology. Science 1988;240:622–630.
8. Weisgraber KH. Apolipoprotein E: structure–function relationships. Adv Prot Chem 1994;45:249–302.
9. Aggerbeck LP, Wetterau JR, Weisgraber, KH, Wu C-SC, Lindgren FT. Human apolipoprotein E3 in aqueous solution. II. Properties of the amino- and carboxyl-terminal domains. J Biol Chem 1988; 263:6249–6258.
10. Wetterau JR, Aggerbeck LP, Rall SC Jr, Weisgraber KH. Human apolipoprotein E3 in aqueous solution. I. Evidence for two structural domains. J. Biol. Chem. 1988;263:6240–6248.
11. Mahley RW, Innerarity TL, Pitas RE, Weisgraber KH, Brown JH, Gross E. Inhibition of lipoprotein binding to cell surface receptors of fibroblasts following selective modification of arginyl residues in arginine-rich and B apoproteins. J Biol Chem 1977;252:7279–7287.
12. Weisgraber KH, Innerarity TL, Mahley RW. Role of lysine residues of plasma lipoproteins in high affinity binding to cell surface receptors on human fibroblasts. J Biol Chem 1978;253:9053–9062.
13. Innerarity TL, Pitas RE, Mahley RW. Binding of arginine-rich (E) apoprotein after recombination with phospholipid vesicles to the low density lipoprotein receptors of fibroblasts. J Biol Chem 1979;254:4186–4190.
14. Wilson C, Wardell MR, Weisgraber KH, Mahley RW, Agard DA. Three-dimensional structure of the LDL receptor-binding domain of human apolipoprotein E. Science 1991;252:1817–1822.
15. De Pauw M, Vanloo B, Weisgraber KH, Rosseneu M. Comparison of lipid-binding and lecithin:cholesterol acyltransferase activation of the amino- and carboxyl-terminal domains of human apolipoprotein E3. Biochemistry 1995;34:10953–10966.
16. Raussens V, Fisher CA, Goormaghtigh E, Ryan RO, Ruysschaert J-M. The low density lipoprotein receptor active conformation of apolipoprotein E. Helix organization in n-terminal domain-phospholipid disc particles. J Biol Chem 1998;273:25825–25830.
17. Raffai R, Weisgraber KH, MacKenzie R, Rupp B, Rassart E, Hirama T, Innerarity TL, Milne R. Binding of an antibody mimetic of the human low density lipoprotein receptor to apolipoprotein E is governed through electrostatic forces. Studies using site-directed mutagenesis and molecular modeling. J Biol Chem 2000;275:7109–7116.
18. Mahley RW, Ji ZS. Remnant lipoprotein metabolism: key pathways involving cell-surface heparan sulfate proteoglycans and apolipoprotein E J Lipid Res 1999;40:1–16.
19. Smith GR, Sternberg MJ. Prediction of protein–protein interactions by docking methods Curr Opin Struct Biol 2002;12:28–35.
20. Russell DW, Brown MS, Goldstein JL. Different combinations of cysteine-rich repeats mediate binding of low density lipoprotein receptor to two different proteins. J Biol Chem 1989;264:21682–21688.
21. Dong LM, Parkin S, Trakhanov SD, Rupp B, Simmons T, Arnold KS, Newhouse YM, Innerarity TL, Weisgraber KH. Novel mechanism for defective receptor binding of apolipoprotein E2 in type III hyperlipoproteinemia. Nat Struct Biol 1996;3:718–722.
22. Raussens V, Slupsky CM, Ryan RO, Sykes BD. NMR structure and dynamics of a receptor-active apolipoprotein E peptide. J Biol Chem 2002;277:29172–29180.
23. Lo Conte L, Chothia C, Janin J. The atomic structure of protein-protein recognition sites. J Mol Biol 1999;285:2177–2198.
24. Betts MJ, Sternberg MJ. An analysis of conformational changes on protein–protein association: implications for predictive docking. Prot Eng 1999;12:271–283.
25. Dolmer K, Huang W, Gettins PGW. NMR solution structure of complement-like repeat CR3 from the low density lipoprotein receptor-related protein. Evidence for specific binding to the receptor binding domain of human alpha(2)-macroglobulin. J Biol Chem 2000;275: 3264–3269.
26. Nielsen KL, Holtet TL, Etzerodt M, Moestrup SK, Gliemann J, Sottrup-Jensen L, Thogersen HC. Identification of residues in alpha-macroglobulins important for binding to the alpha2-macroglobulin receptor/low density lipoprotein receptor-related protein J Biol Chem 1996;271:12909–12912.
27. Huang W, Dolmer K, Liao X, Gettins PGW. NMR solution structure of the receptor binding domain of human alpha(2)-macroglobulin. J Biol Chem 2000;275:1089–1094.
28. Raffaï R, Maurice R, Weisgraber K, Innerarity T, Wang X, MacKenzie R, Hirama T, Watson D, Rassart E, Milne R. Molecular characterization of two monoclonal antibodies specific for the LDL receptor-binding site of human apolipoprotein E. J Lipid Res 1995;36:1905–1918.
29. Rudenko G, Henry L, Henderson K, Ichtchenko K, Brown MS, Goldstein JL, Deisenhofer J. Structure of the LDL receptor extracellular domain at endosomal pH. Science 2002;298:2353–2358.
30. Gabb HA, Jackson RM, Sternberg MJ. Modeling protein docking using shape complementarity, electrostatics and biochemical information. J Mol Biol 1997;272:106–120.

31. Moont G, Gabb HA, Sternberg MJ. Use of pair potentials across protein interfaces in screening predicted docked complexes Proteins 1999;35:364–373.
32. Brooks BR, Bruccoleri RE, Olafsson D, States D, Swaminathan S, Karplus M. (1983) CHARMM: a program for macromolecular energy minimization, and dynamics calculations J Comput Chem 1983;4:187–217.
33. Dominy BN, Brooks CL. III Development of a generalized Born model parametrization for proteins and nucleic acids. J Chem Phys B 1999;103:3765–3773.
34. Madura JD, Briggs JM, Wade RC, Davis ME, Luty BA, Ilin A, Antosiewicz J, Gilson MK, Bagheri B, Scott LR, McCammon JA. Electrostatic and diffusion in solution: Simulations with the University of Houston Brownian dynamics program. Comp Phys Commun 1995;91:57–95.
35. Schaefer M, van Vlijmen HWT, Karplus M. Electrostatic contributions to molecular free energies in solution. Adv Protein Chem 1998;51:1–57.
36. Antosiewicz J, McCammon JA, Gilson MK. Prediction of pH-dependent properties of proteins. J Mol Biol 1994;238:415–436.
37. Bashford D. Scientific computing in object-oriented parallel environments. In: Ishikawa, Y, Oldehoeft RR, Reynders JVW, Tholburn M, editors. Lecture Notes in Computer Science, vol. 1243. Berlin: ISCOPE97, Springer; 1997. p 233–240.
38. Alard P. Computations of surface areas and energies in the field of macromolecules. PhD thesis. Universitè Libre de Bruxelles, Belgium, 1991.
39. Delhaise P, Van Belle D, Bardiaux M, Alard P, Hamers P, Van cutsem E, Wodak SJ. Analysis of data from computer simulations on macromolecules using the ceram package. J Mol Graph 1985;3: 116–119.
40. Lalazar A, Weisgraber KH, Rall SC Jr, Giladi H, Innerarity TL, Levanon AZ, Boyles JK, Amit B, Gorecki M, Mahley RW. Site-specific mutagenesis of human apolipoprotein E. Receptor binding activity of variants with single amino acid substitutions. J Biol Chem 1988;263:3542–3545.
41. Zaiou M, Arnold KS, Newhouse YM, Innerarity TL, Weisgraber KH, Segall ML, Phillips MC, Lund-Katz S. Apolipoprotein E low density lipoprotein receptor interaction. Influences of basic residue and amphipathic alpha-helix organization in the ligand J Lipid Res 2000;41:1087–1095.
42. Lund-Katz S, Zaiou M, Wehrli S, Dhanasekaran P, Baldwin F, Weisgraber KH, Phillips M C. Effects of lipid interaction on the lysine microenvironments in apolipoprotein E J Biol Chem 2000; 275:34459–34464.
43. Raussens V, Mah MKH, Kay CM, Sykes BD, Ryan RO. (2000) Structural characterization of a low density lipoprotein receptor-active apolipoprotein E peptide, ApoE3-(126–183). J Biol Chem 2000;275:38329–38336.
44. Rooman M, Kocher J-P, Wodak SJ. Extracting information on folding from the amino acid sequence: accurate predictions for protein regions with preferred conformation in the absence of tertiary interactions. Biochemistry 1992;31:10226–10238.
45. North CL, Blacklow SC. Evidence that familial hypercholesterolemia mutations of the LDL receptor cause limited local misfolding in an LDL-A module pair. Biochemistry 2000;39:13127–13135.
46. Burley SK, Petsko GA. Amino–aromatic interactions in proteins. FEBS Lett 1986;203:139–143.
47. Prèvost M. Concurrent interactions contribute to the raised pKa of His18 in barnase J Mol Biol 1996;260:99–110.
48. Hussain MM, Strickland DK, Bakillah A. The mammalian low-density lipoprotein receptor family. Annu Rev Nutr 1999;19:141–172.
49. Bu G, Marzolo MP. Role of rap in the biogenesis of lipoprotein receptors. Trends Cardiovasc Med 2000;10:148–155.
50. Databases for FH mutations: www.ucl.ac.uk and www.umd.necker.fr
51. Morrow JA, Arnold KS, Dong J, Balestra ME, Innerarity TL, Weisgraber KH. Effect of arginine 172 on the binding of apolipoprotein E to the low density lipoprotein receptor. J Biol Chem 2000;275:2576–2580.
52. Bieri S, Atkins AR, Lee HT, Winzor DJ, Smith R, Kroon PA. Folding, calcium binding, and structural characterization of a concatemer of the first and second ligand-binding modules of the low-density lipoprotein receptor. Biochemistry 1998;37:10994–11002.
53. Beglova N, North CL, Blacklow SC. Backbone dynamics of a module pair from the ligand-binding domain of the LDL receptor. Biochemistry 2001;40:2808–2815.